

Journal of Nanophotonics

SPIEDigitalLibrary.org/jnp

Absorption enhancement in thin-film silicon solar cells by two-dimensional periodic nanopatterns

Shaomin Wu
Wei Wang
Kitt Reinhardt
Yalin Lu
Shaochen Chen



Absorption enhancement in thin-film silicon solar cells by two-dimensional periodic nanopatterns

Shaomin Wu,^a Wei Wang,^a Kitt Reinhardt,^b Yalin Lu,^c
and Shaochen Chen^d

^aThe University of Texas at Austin, Materials Science and Engineering, Austin, TX 78712
wushaomin@yahoo.com

^bUnited States Air Force Office of Scientific Research, AFOSR/NE, 875 North Randolph
Street, Suite 326, Arlington, VA 22203

^cUnited States Air Force Academy, Physics Department, Laser Optics Research Center,
Colorado Springs, CO 80840

^dThe University of Texas at Austin, Mechanical Engineering Department, Austin, TX 78712
scchen@mail.utexas.edu

Abstract. A major problem of current silicon thin film solar cells lies in low carrier collection efficiency due to short carrier diffusion length. Instead of improving the collection efficiency in a relatively thick solar cell, increasing light absorption while still keeping the active layer thin is an alternative solution. Absorption enhancement in a thin film Si solar cell by incorporating a two-dimensional periodic metallic nanopattern was investigated using three-dimensional finite element analysis. By studying the enhancement effect brought by different materials, dimensions, coverage, and dielectric environments of the metal nanopattern, we found that absorption enhancement occurs at wavelength range outside surface plasmons resonance of the nanostructures. The exploitation of the nanostructures also enhances the Fabry-Perot resonance in the active layer. It plays an important role in optimizing the absorption of the solar cell.

Keywords: surface plasmons, nonresonant scattering, finite element, absorption enhancement, solar cells.

1 INTRODUCTION

Silicon thin-film solar cells have attracted an extensive research interest due to a significant cost advantage over their bulk crystalline predecessors. Yet, before thin-film solar cells can become a competitive candidate as a major solar energy source, the efficiency must be increased. The main challenge for improving the efficiency lies in the fact that the material used in the active region of a thin-film solar cell is usually either polycrystalline or amorphous. The carrier life time (τ) in such materials is quite low. This results in a short diffusion length $L = \sqrt{D \cdot \tau}$. Therefore, expectation of both efficient carrier collection and low cost production will prefer the use of a thin layer of light absorbing material. On the other hand, the light absorbing material has to be thick enough to ensure maximum carrier generation. Instead of improving the charge collection efficiency using a relatively thick solar cell, increasing the light absorption while still keeping the active layer thin will be an alternative way to resolve this dilemma. One of the well-known and most commonly used methods for absorption enhancement is the use of scattering surface textures [1] for light trapping. However, this is not a viable option for thin-film solar cells because the roughness of these surface textures is of the same order as the thickness of the thin-film active layer. Increased surface recombination resulting from an enlarged surface area will deteriorate the overall cell performance.

Recently, the idea of employing nanoscale metallic materials to improve the light absorption of solar cells has been gaining attention. Early work, such as the incorporation of small copper or silver clusters in an organic solar cell to increase the photovoltaic conversion efficiency, was done by Stenzel and Westphalen [2-3] in the late 1990s. An increase in the short circuit current by a factor of 2 was reported. In the past few years, gold or silver nanoparticles with sizes ranging from tens of nanometers to over a hundred nanometers were introduced to both crystalline [4-5] and amorphous [6] silicon solar cells. Enhancement in both photocurrent and conversion efficiency were experimentally observed. All of such performance improvements were attributed to light scattering by surface plasmons (SP). However, a latest study by Pala has shown that the previous observation may not be only from the SP effect [7]. Because that current computer technology has made simulation of electromagnetic (EM) field on many sophisticated nanoscale structures possible, various plasmonic nanostructures have been proposed, and their potential in improving solar cell performance has been investigated [8-11]. Most of such work, however, were numerical analyses on two-dimensional structures and considered only one polarization of an incident light. This not only restricts their designs to one-dimensional plasmonic structures such as nanowires or nanogratings, but is also insensitive to the randomly polarized nature of solar radiation.

To establish a more realistic analysis, this paper is focused on a three-dimensional (3D) thin-film plasmonic solar cell model with a periodic metal nanoparticle array incorporated. The periodic pattern not only facilitates the setting of boundary conditions in simulation, but also allows an in-depth investigation of absorption enhancement effects from a single nanoparticle and multiple particles simultaneously. By simulating the EM field in a chosen model structure using 3D finite element analysis, we were able to study such effects from incorporating various nanopatterns. These results were used to identify different enhancement mechanisms and derive the criteria for optimizing a nanostructure-enhanced thin-film solar cell.

2 COMPUTATIONAL DETAILS

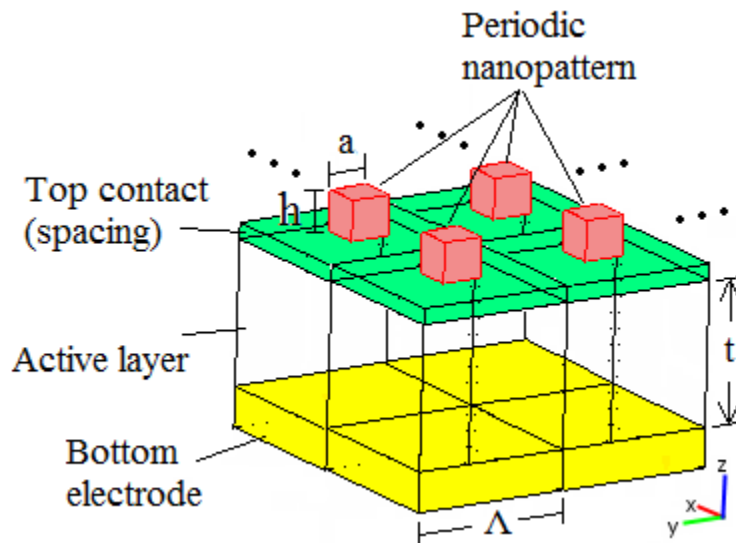


Fig. 1. Structure of the nanopattern incorporated solar cell model to be used in simulation.

Figure 1 shows a typical Si thin-film solar cell structure with a periodic nanopattern on top. This structure was simulated in COMSOL Multiphysics, a commercial 3D finite element analysis software. In this model, amorphous Si (a-Si) was chosen as the active material.

Compared to polycrystalline Si, a-Si has a larger absorption rate, and thus is more suitable to be used as a light absorbing material in a nanoscale device. An Al film with thickness fixed at 100 nm was placed underneath the active layer as the bottom electrode. In a real a-Si solar cell, the bottom electrode is usually much thicker and might be other metal materials. Having tried materials, such as Au, Ag, Ti, and other thickness values that are larger than 100 nm for the bottom electrode, we observed no difference on the optical performance of the solar cell within the wavelength range of interests. Either as a top contact or as a passivation layer, a dielectric spacing layer was introduced between the nanoparticle array and the a-Si film. The incident solar radiation was assumed to be along z -axis with electric field polarized to the x direction. Since solar radiation is equally distributed in either one of the two polarizations, the dimension, geometry, and optical properties of the nanopattern were set to be identical in both x and y , so that only one polarization of the incident light needs to be considered for this study. By setting periodic boundary conditions on four faces surrounding each repeating unit in the x and y dimensions, the whole structure can be simplified into one unit. Perfectly matched layers (PML) were used to eliminate unnecessary reflection at the top and bottom boundaries of the simulated domain. The dielectric constant data were taken from Refs. 12 and 13.

Based on the Poynting theorem, the time-averaged power being absorbed in the active material is

$$Absorption = \frac{1}{2} \sigma \cdot \int_V |\bar{E}|^2 \cdot dV, \quad (1)$$

where \bar{E} is the steady-state electric field, V is the volume of the active layer and the $\sigma = \omega \cdot \text{Im}(\epsilon)$ is the product of the frequency of the oscillating electric field and the imaginary part of the dielectric constant. To calculate the absorption enhancement $\kappa(\lambda)$ at different wavelengths,

$$\begin{aligned} \kappa(\lambda) &= \frac{Absorption (solar cell with nanopattern)}{Absorption (same solar cell without nanopattern)} \\ &= \frac{\int_V |\bar{E}|^2 \cdot dV \Big|_{with \ nanopattern}}{\int_V |\bar{E}|^2 \cdot dV \Big|_{without \ nanopattern}} \end{aligned} \quad (2)$$

a reference solar cell with the same structure except the nanopattern on top was introduced. An enhancement value greater than one means absorption in the active layer is increased due to the presence of the nanostructure. Considering the energy distribution spectrum of solar energy and the spectral response of the solar cell, the wavelength range of interest was chosen to be from the ultraviolet to near infrared. The following components were varied to identify possible enhancement mechanisms: the lateral dimension a and the vertical dimension h of each nanoparticle, the period Λ , the material and dielectric environment of the nanoparticle array, and thickness t of the photoactive material.

3 RESULTS AND DISCUSSION

The nanopattern-induced absorption enhancement with respect to the wavelength of the incident light in a particular solar cell structure is shown in Figure 2(a). In this model, the a-Si layer thickness was chosen to be 160 nm. The reasons to select this thickness are not only to consider the optical absorption rate of a-Si material in order to leave enough room for enhancement, but also to allow for a possible observation of different enhancement mechanisms. The nanopattern has a period of 100 nm and each nanoparticle is 50 nm in all three dimensions. This array is placed on top of the active region with a 20 nm thick Indium Tin Oxide (ITO) in between as a contact layer. Nanoparticle arrays of three different

materials, Ag, Al and Au, were studied. All of the three enhancement curves show two common features, a peak and a valley centered at about 990 nm and 870 nm respectively. This is attributed to the Fabry-Perot cavity resonance within the a-Si film with the peak and the valley corresponding to the constructive and the destructive interference respectively. As the thickness of a-Si layer was reduced to 140 nm (Figure 2(b)) and 120 nm (Figure 2(c)), such common peaks and valleys blue-shifted. It is understandable according to the changed cavity length.

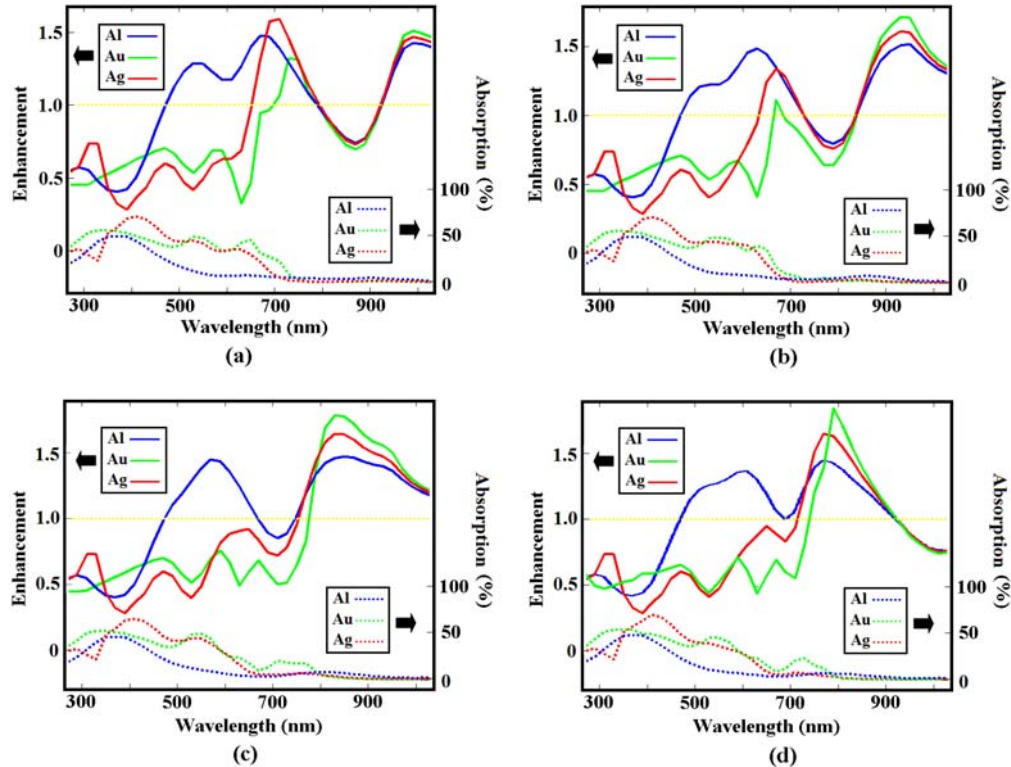


Fig. 2. Spectral absorption rate (dotted line) of Al, Au, Ag nanoparticles array and absorption enhancement spectrum (solid line) in the active layer brought by the nanopatterns: $a = h = 50$ nm, $A = 100$ nm. An enhancement value greater than one (above the yellow dotted line) means an increase in the optical absorption within the active region. The thickness of a-Si layer t is 160 nm in (a), 140 nm in (b), 120 nm in (c) and 200 nm in (d).

The cause of the enhancement peaks in the wavelength range of visible light in Figures 2(a)-(c) is not as straightforward as those common peaks. We will show that it is a combined effect of the enhanced light scattering by the nanoparticles and the interference of the scattered light inside the a-Si Fabry-Perot cavity. Metallic nanostructures are known to be capable of scattering light with a scattering cross-section larger than their own size through excitation of SP [14]. At the same time, enhanced near field associated with the SP resonance also causes extraordinary optical absorption by the nanostructures themselves. This fact is confirmed by the spectral absorption rate of the nanopattern, also shown in Figures 2(a)-(c). Strong optical absorption by the nanopattern of each material always emerges in the vicinity of its SP resonance wavelength. As a result, a considerable portion of the incident power is dissipated in the nanoparticles before scattered into the photoactive material underneath. This explains why the absorption enhancement in the active layers is always less than one at the wavelength range where strong absorption in the nanostructure occurs. For Ag and Au

nanopatterns, since their SP resonance lies in the visible light region, the enhancement bandwidth appears to be narrow. In contrast, Al particles have a much wider enhancement range, because their resonant wavelength is in the ultraviolet region. Similar results were also reported by other researcher recently [15]. An important feature in the relatively wide enhancement band of the Al nanopattern shown in Fig 2(a) is the valley at 600 nm. The mechanism behind is the destructive interference of nanostructure scattered light inside the thin a-Si cavity. It is the superposition of the destructive minimum on the enhancement band of the Al nanoparticles in the visible region that splits the enhancement band into two peaks. As can be seen in Figures 2(b) and (c), the destructive minimum blue-shifts and eventually moves out of the Al enhancement band, with the decreasing thickness of the a-Si layer. Same phenomena were not observed for the Ag and Au nanopattern in the same region, since their enhancement bandwidth is relatively narrow. However, the suppression of their enhancement peaks by the destructive interference can still be clearly observed in both Figures 2(b) and (c).

Based on the discussion above, one way to expand the bandwidth of the enhancement is to push the common valley at 870 nm in Figure 2(a) to even longer wavelength. This can be achieved by increasing the thickness of the a-Si layer. Shown in Figure 2(d), as the active layer becomes 200nm thick, the bandwidth of three enhancement curves all substantially increased. However, since the absorption of a-Si vanishes beyond 800 nm and most of the solar energy lies in the visible band, extending the enhancement band towards infrared does little contribution to the efficiency of the solar cells. The key is to extend the enhancement band towards shorter wavelength, especially for Ag and Au nanoparticles. Shrinking the size of the nanoparticles to blue-shift the SP resonance is a reasonable thought. Figure 3(a) shows the enhancement and absorption spectra of the three nanopatterns when the lateral dimension of each nanoparticle decreases from 50 nm to 30 nm. To minimize the influence of the destructive interference to the absorption enhancement in the active layer, we set the thickness of the a-Si film to be 60nm only. Not surprisingly, the SP resonance wavelengths all blue-shift. Consequently, the enhancement band of all three materials expands towards the shorter wavelength. Although the density of the nanoparticles remained unchanged as we cut the lateral dimension of the nanoparticles, the coverage which is the percentage of the area covered by the metallic nanoparticles was reduced. Compared with the 50 nm wide nanoparticles (not shown), the lower coverage of the 30 nm nanoparticles directly gives rise to the significant drop of the enhancement intensity in Figure 3(a). Shown in Figure 3(b), for the nanoparticles with the same sizes, when they are placed far apart, there is hardly any interaction of the SPs between adjacent particles. Changing the coverage only affects the enhancement intensity, but not the enhancement wavelength range. As the edge-to-edge distance of the nanoparticles falls below 25 nm, multiple-scattering effect of SPs becomes noticeable [16], resulting in a red-shift of the SP resonance wavelength and a correspondingly narrowed enhancement bandwidth.

The SP resonance wavelength of a nanoscale object is also highly sensitive to its dielectric environment. As shown in Figure 3(c), replacing the ITO spacing layer by SiO₂ (a material with smaller dielectric constant), a substantial blue-shift of the SP peak can be observed in the absorption rate curve. Given the large enhancement wavelength tuning range, considerations on the dielectric layer placed between the nanopattern and the active material is also important in designing the nanostructure-enhanced solar cells. Figure 3(d) shows a cross-sectional view of steady-state magnetic field distribution in a 60 nm thick a-Si film with 50 nm wide Al nanoparticle array on top. The simulated field is the y-direction magnetic field H_y with a wavelength of 590 nm. The intensity of the field is normalized to the incident radiation. Although not at the resonance wavelength, strong charge oscillation in x-direction are still excited by the incident light with the electric field polarized in x-direction. This can be evidenced by the intense y-direction magnetic field H_y concentrated at the interface of the nanoparticle and the ITO layer. The stripes inside the a-Si layer are an indication of Fabry-Perot interference within the a-Si cavity.

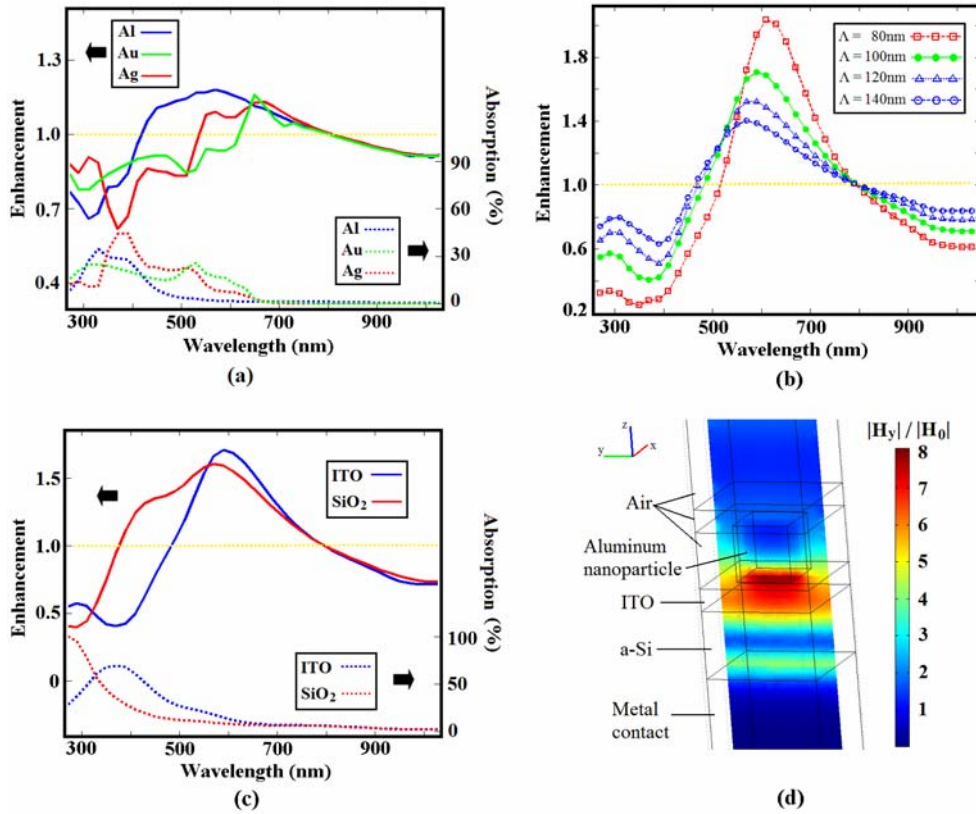


Fig. 3. (a) Absorption enhancement spectrum (solid line) and absorption rate (dotted line) of Al, Au, Ag nanoparticles array: $a = 30$ nm, $h = 50$ nm, $t = 60$ nm, $\Lambda = 100$ nm. (b) Absorption enhancement of Al nanopattern with varying period Λ ($a = h = 50$ nm, $t = 60$ nm). (c) Absorption enhancement spectrum (solid line) and absorption rate (dotted line) of Al nanoparticles array ($\Lambda = 100$ nm, $a = h = 50$ nm, $t = 60$ nm) with 20 nm ITO or SiO₂ spacing layer. (d) A cross-sectional view of the normalized field magnitude for the 3D structure ($\Lambda = 100$ nm, $a = h = 50$ nm, $t = 60$ nm).

As to a real solar cell, it is more important to evaluate the electrical output performance. For an a-Si solar cell that is thin enough to assume 100% charge collection efficiency, the increase in short-circuit current can be calculated as

$$\alpha = \frac{\int_0^{\infty} \kappa(\lambda) \cdot A(\lambda) \cdot I(\lambda) \cdot d\lambda}{\int_0^{\infty} A(\lambda) \cdot I(\lambda) \cdot d\lambda}, \quad (3)$$

where $\kappa(\lambda)$ is the absorption enhancement obtain from the simulation of a specific nanopattern enhanced solar cell structure, $A(\lambda)$ is the absorption rate of the active layer for the reference solar cell without any nanoparticles, and $I(\lambda)$ is the incident photon flux converted from the AM1.5G solar radiation spectrum. If the device has less than ideal carrier collection efficiency, the quantum efficiency $\eta(\lambda)$ needs to be considered. The photocurrent enhancement becomes

$$\alpha = \frac{\int_0^{\infty} \kappa(\lambda) \cdot A(\lambda) \cdot \eta(\lambda) \cdot I(\lambda) \cdot d\lambda}{\int_0^{\infty} A(\lambda) \cdot \eta(\lambda) \cdot I(\lambda) \cdot d\lambda}. \quad (4)$$

The quantum efficiency data can be taken from Ref. 17. The quantum efficiency may change depending on specific device structures, however, the resulting α will not change as long as the shape of the $\eta(\lambda)$ vs. λ curve remains the same. The Al nanoparticle array corresponding to the blue curve in Figure 2(d) can easily give a 20% enhancement in photocurrent.

4 CONCLUSION

Absorption enhancement in a thin-film Si solar cell by incorporating a two-dimensional metallic nanoparticle array was studied using 3D finite element analysis. We have identified two different enhancement mechanisms and considered the influences of the active layer thickness and the material, dimension, coverage, and dielectric environment of the metallic nanopattern in order to demonstrate a way to optimize the nanostructure for maximum solar cell performance improvement. Suffering from the high energy dissipation in the visible range, the Ag and Au nanopatterns did not provide good absorption enhancement to the solar cells. On the other hand, Al nanoparticles array brought considerable increase in absorption although they were not in SP resonance at the wavelength of highest enhancement. By considering photon distribution of the solar radiation, the quantum efficiency and the absorption rate of active material, a 20% increase of the photocurrent can be easily achieved. Using the same designing method, the nanopattern can also be applied to other thin-film solar cells with different light absorbing materials such as Copper indium gallium selenide (CIGS), CdTe and even organic films.

Acknowledgments

Financial support from the Air Force Office of Scientific Research, National Science Foundation, and the Office of Naval Research is greatly appreciated. S. C. is grateful for the computer support from Intel's Higher Education Program.

References

- [1] M. A. Green, "Lambertian light trapping in textured solar cells and light-emitting diodes: analytical solutions," *Prog. Photovolt. Res. Appl.* **10**, 235-241 (2002) [doi:10.1002/pip.404].
- [2] O. Stenzel, A. Stendal, K. Voigtsberger, and C. von Borczykowski, "Enhancement of the photovoltaic conversion efficiency of copper phthalocyanine thin film devices by incorporation of metal clusters," *Sol. Energy Mater. Sol. Cells* **37**, 337-348 (1995) [doi:10.1016/0927-0248(95)00027-5].
- [3] M. Westphalen, U. Kreibig, J. Rostalski, H. Lüth, and D. Meissner, "Metal cluster enhanced organic solar cells," *Sol. Energy Mater. Sol. Cells* **61**, 97-105 (2000) [doi:10.1016/S0927-0248(99)00100-2].
- [4] S. Pillai, K. R. Catchpole, T. Trupke, and M. A. Green, "Surface plasmon enhanced silicon solar cells," *J. Appl. Phys.* **101**, 093105 (2007) [doi:10.1063/1.2734885].
- [5] D. M. Schaadt, B. Feng, and E. T. Yu, "Enhanced semiconductor optical absorption via surface plasmon excitation in metal nanoparticles," *Appl. Phys. Lett.* **86**, 063106 (2005) [doi:10.1063/1.1855423].
- [6] D. Derkacs, S. H. Lim, P. Matheu, W. Mar, and E. T. Yu, "Improved performance of amorphous silicon solar cells via scattering from surface plasmons polaritons in nearby metallic nanoparticles," *Appl. Phys. Lett.* **89**, 093103 (2006) [doi:10.1063/1.2336629].
- [7] R. A. Pala, J. White, E. Barnard, J. Liu, and M. L. Brongersma, "Design of plasmonic thin-film solar cells with broadband absorption enhancements," *Adv. Mater.* **21**, 1-6 (2009) [doi:10.1002/adma.200900331].

- [8] K. R. Catchpole and A. Polman, "Design principles for particle plasmon enhanced solar cells," *Appl. Phys. Lett.* **93**, 191113 (2008) [doi:10.1063/1.3021072].
- [9] C. Rockstuhl, S. Fahr and F. Lederer, "Absorption enhancement in solar cells by localized plasmon polaritons," *J. Appl. Phys.* **104**, 123102 (2008) [doi:10.1063/1.3037239].
- [10] V. E. Ferry, L. A. Sweatlock, D. Pacifici and H. A. Atwater, "Plasmonic nanostructure design for efficient light coupling into solar cells," *Nano Lett.* **8**, 4391-4397 (2008) [doi:10.1021/nl8022548].
- [11] W. Wang, S. Wu, K. Reinhardt, Y. Lu, and S. C. Chen, "Broadband Light Absorption Enhancement in Thin-Film Silicon Solar Cells," *Nano Lett.* **10**, 2012-2018 (2010) [doi:10.1021/nl904057p].
- [12] E. D. Palik, *Handbook of Optical Constants of Solids, Vol. 1*, 290 pp., Academic, San Diego, CA (1985).
- [13] D. Mergel and Z. Qiao, "Dielectric modelling of optical spectra of thin In₂O₃:Sn films," *J. Phys. D* **35**, 794-801 (2002) [doi:10.1088/0022-3727/35/8/311].
- [14] C. F. Bohren and D. R. Huffman, *Absorption and Scattering of Light by Small Particles*, Wiley, New York (1998) [doi:10.1002/9783527618156].
- [15] Y. A. Akimov and W. S. Koh, "Resonant and nonresonant plasmonic nanoparticle enhancement for thin-film silicon solar cells," *Nanotechnology* **21**, 235201 (2010) [doi:10.1088/0957-4484/21/23/235201].
- [16] L.-H. Han, W. Wang, Y. Lu, R. J. Knize, K. Reinhardt, J. R. Howell, and S. C. Chen, "Analytical and experimental investigation of electromagnetic field enhancement among nanospheres with varying spacing," *ASME J. Heat Transf.* **131**, 033110 (2009) [doi:10.1115/1.3056574].
- [17] J. Meier, J. Spitznagel, U. Kroll, C. Bucher, S. Fay, T. Moriarty and A. Shah, "High-efficiency amorphous and 'micromorph' silicon solar cells," *Proc. 3rd World Conf. PVSEC, Osaka, Japan*, **3**, 2801-2805 (2003).